

Slip Rate on the San Diego Trough Fault Zone, Inner California Borderland, and the 1986 Oceanside Earthquake Swarm Revisited

by H. F. Ryan, J. E. Conrad, C. K. Paull, and M. McGann

Abstract The San Diego trough fault zone (SDTFZ) is part of a 90-km-wide zone of faults within the inner California Borderland that accommodates motion between the Pacific and North American plates. Along with most faults offshore southern California, the slip rate and paleoseismic history of the SDTFZ are unknown. We present new seismic reflection data that show that the fault zone steps across a 5-km-wide stepover to continue for an additional 60 km north of its previously mapped extent. The 1986 Oceanside earthquake swarm is located within the 20-km-long restraining stepover. Farther north, at the latitude of Santa Catalina Island, the SDTFZ bends 20° to the west and may be linked via a complex zone of folds with the San Pedro basin fault zone (SPBFZ). In a cooperative program between the U.S. Geological Survey (USGS) and the Monterey Bay Aquarium Research Institute (MBARI), we measure and date the coseismic offset of a submarine channel that intersects the fault zone near the SDTFZ–SPBFZ junction. We estimate a horizontal slip rate of about 1.5 ± 0.3 mm/yr over the past 12,270 yr.

Introduction

The inner California Borderland is cut by numerous faults subparallel to the San Andreas fault that exhibit complex histories and styles of deformation including strike-slip faults and blind thrusts (e.g., Fisher *et al.*, 2009). Faults within the inner Continental Borderland take up as much as 20% of the slip between the Pacific and North American plates (DeMets and Dixon, 1999). Geodetic data show 8 mm/yr of predominantly strike-slip motion on offshore Borderland faults east of San Clemente Island (Platt and Becker, 2010). Many offshore faults lack the critical information needed for use in seismic hazard assessments such as slip rate, demonstrated Holocene offset, and earthquake recurrence intervals. Thus, few offshore faults have been included in the Working Group of California Earthquake Probabilities (WGCEP) Uniform California Earthquake Rupture Forecast (UCERF) (e.g., Field, 2007).

The focus of this study is on the San Diego trough fault zone (SDTFZ), one of several northwest-trending right-lateral fault zones mapped between San Clemente Island and the mainland in the offshore California Borderland (Fig. 1). Other major subparallel strike-slip faults accommodating some of the 8 mm/yr slip include the Newport–Inglewood–Rose Canyon fault zone; the Palos Verdes fault zone, which is north of and along strike with the Coronado Bank fault zone; and the San Clemente fault zone, which is west of the SDTFZ (Fig. 1). Both the Newport–Inglewood–Rose Canyon

and Palos Verdes fault zones extend on land where they have measured slip rates; the Rose Canyon fault zone has a minimum slip rate of 1.0 mm/yr (Lindvall and Rockwell, 1995), and the Palos Verdes fault zone has a rate of ~3 mm/yr (McNeilan *et al.*, 1996).

Because the Newport–Inglewood–Rose Canyon and Palos Verdes fault zones have known slip rates, these faults are generally included in hazard studies (Field, 2007) and as bounding blocks in geodetic models of plate motions in southern California (e.g., McCaffrey, 2005; Meade and Hager, 2005a). However, the use of the Palos Verdes fault zone as a main throughgoing fault in these models may not be correct as recent mapping indicates that it does not connect with the Coronado Bank fault zone to the south but terminates south of Lasuen Knoll (Fig. 2; Conrad *et al.*, 2010). Thus, other fault zones in the offshore need to be considered for inclusion in hazard and geodetic modeling studies to account for the geodetically determined slip on offshore faults. One of these faults is the SDTFZ.

In this paper, we use recently developed ultra-high-resolution seafloor surveying and sampling techniques developed at the Monterey Bay Aquarium Research Institute (MBARI) to estimate a Holocene slip rate for the SDTFZ. This is the first slip rate determined for a fault that lies entirely offshore in the Borderland. In addition, we present high-resolution seismic reflection profiles that show that the

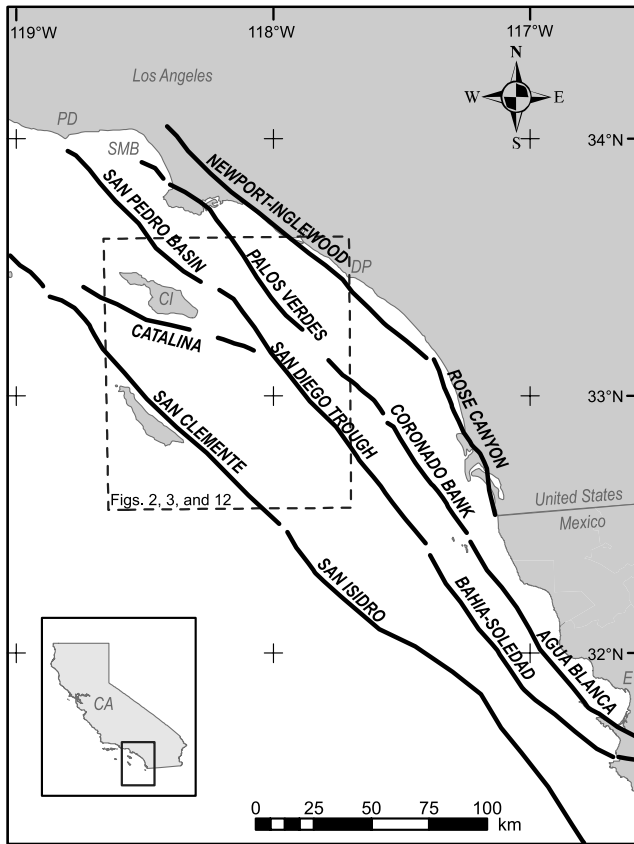


Figure 1. Simplified fault map of major northwest-trending offshore strike-slip faults. The faults offshore of Mexico are modified from Legg *et al.* (1991); the faults offshore of California are modified from the California Geological Survey (CGS, 2006) and from this study. CI, Santa Catalina; Island; DP, Dana Point; E, Ensenada; PD, Point Dume; and SMB, Santa Monica Bay.

SDTFZ extends 60 km farther north of where it was previously mapped, possibly joining the San Pedro Basin fault zone (SPBFZ). A combined SDTFZ–SPBFZ has a length of 260 km and appears to be one of the most active fault zones in the Borderland.

Previous Work

The SDTFZ was first thought to extend from the U.S.–Mexico border to just south of Crespi Knoll based on seismic reflection profiling (Fig. 2; Moore, 1969). The fault zone was mapped in greater detail by Kennedy *et al.* (1979), Legg and Kennedy (1979), Legg (1991), and Legg *et al.* (1991). About 30 km west of San Diego, the SDTFZ runs along the axis of the San Diego trough, an 1100-m deep basin that lies between the Thirtymile and Coronado Banks (Fig. 2). Here the trend of the SDTFZ is linear with an orientation of N30°W. Dextral strike-slip motion within the SDTFZ is inferred by the relatively simple, straight trace of the fault, which shows alternating east and west side up scarps along strike (Legg, 1991; Legg *et al.*, 1991). The fault zone is generally composed of one or two high-angle fault strands that cut through Quaternary sediment at or just

beneath the seafloor. South of the Mexican border, the SDTFZ continues for about 45 km where it joins with the Bahia Soledad fault zone (Fig. 1) in a complex manner; the Bahia Soledad fault zone connects with the onshore Agua Blanca fault zone south of Ensenada, Baja California (Legg, 1991; Legg *et al.*, 1991). The northern extent of the SDTFZ is more complicated. One interpretation shows the SDTFZ making a sharp bend to the west near Crespi Knoll and merging with the Catalina fault zone (Legg, Borrero, and Synolakis, 2004; Legg *et al.*, 2007). Another interpretation shows the SDTFZ continuing north toward the SPBFZ (Ryan *et al.*, 2009; Francis and Legg, 2010).

Data

During cruises conducted between 2008 and 2010, the U.S. Geological Survey (USGS) collected high-resolution single channel seismic reflection profiles between La Jolla fan valley and Catalina Island (Fig. 3). The source was a SIG 2Mille minisparker, operated at a power of 500 J and repetition rate of 1.75/s. The frequency ranged between 200 and 1000 Hz. These data were supplemented by high-resolution multichannel seismic (MCS) air gun reflection and single channel deep-tow boomer data previously acquired by the USGS from 1998 to 2000 (Normark *et al.*, 1999; Gutmacher *et al.*, 2000; Sliter *et al.*, 2005) and deep penetration industry MCS data collected in the late 1970s and early 1980s available at the National Archive of Marine Seismic Surveys (see Data and Resources).

Gravity cores were collected at several sites along the SDTFZ in order to date sedimentary layers offset by faulting. Nineteen sediment samples from five cores were dated by accelerator mass spectrometry (AMS) carbon-14 (¹⁴C) using a mixed planktic foraminifera assemblage of mostly *Neogloboquadrina pachyderma*, *Globigerina bulloides*, and *N. dutertrei* (Table 1). Calibrated ages and offset measurements were used to determine the fault slip rate. Radiocarbon dating was provided by the National Ocean Sciences AMS (NOSAMS) facility at the Woods Hole Oceanographic Institution. A 633-yr reservoir age was used for the planktic foraminiferal samples (Stuiver and Braziunas, 1993; Ingram and Southon, 1996; Kennett *et al.*, 2000). The raw radiocarbon ages were then converted to calibrated ages using the CALIB 5.0.1 program (Stuiver and Reimer, 1993).

Two sites along the SDTFZ were selected for ultra-high-resolution MBARI automated underwater vehicle (AUV) surveys. One site is located within a restraining stepover area and the other along a channel that is offset horizontally by the SDTFZ (Fig. 3). The AUV carries a Reson 7100, 200-kHz multibeam sonar and an Edgetech 2- to 16-kHz chirp sub-bottom profiler (Caress *et al.*, 2008). The AUV was preprogrammed to proceed to > 200 waypoints during each dive. Missions were up to 18 hr in duration and were designed for the vehicle to fly at a speed of 3 knots while maintaining an altitude of 50 m above the seafloor. Tracklines were spaced at ~150 m apart in order to obtain overlapping multibeam

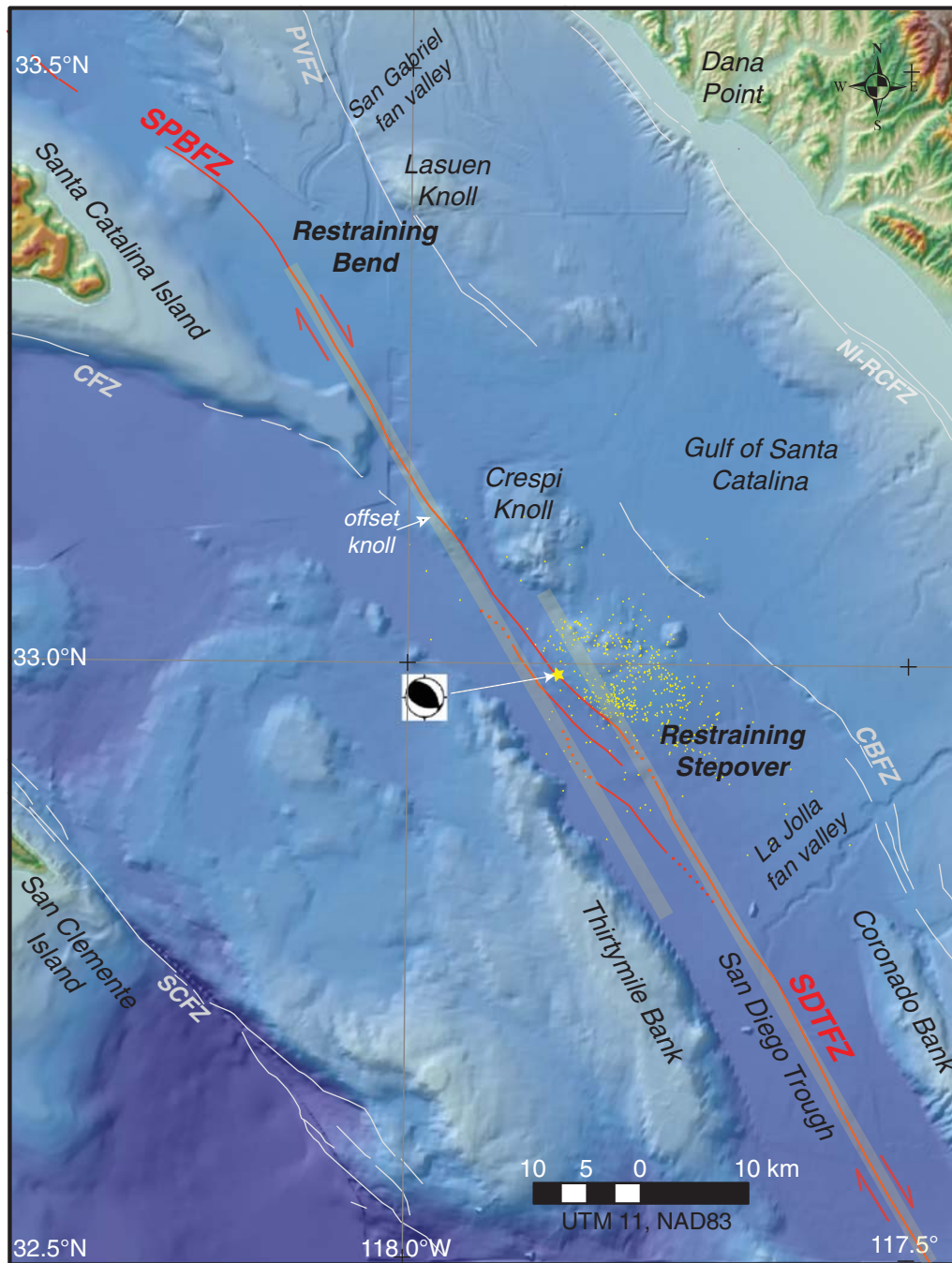


Figure 2. Bathymetric map of the inner Continental Borderland showing locations of structures associated with the SDTFZ including fault strands shown in red (dotted where buried). Other faults are from the [CGS \(2006\)](#) and include the following: San Pedro Basin fault zone (SPBFZ), Newport–Inglewood–Rose Canyon fault zone (NI–RCFZ), Palos Verdes fault zone (PVFZ), Coronado Bank fault zone (CBFZ), Catalina fault zone (CFZ), and San Clemente fault zone (SCFZ). The semitransparent yellow lines are oriented N30°W and offset from each other by 5 km. The star denotes the epicenter of the 1986 Oceanside earthquake with yellow dots showing aftershocks with $M > 2.5$ ([Astiz and Shearer, 2000](#)). The focal mechanism is from [Hauksson and Jones \(1988\)](#). The location of the figure shown in Figure 1.

bathymetric coverage. Resulting bathymetry data had a vertical resolution of 0.15 m and a horizontal footprint of 0.7 m. The chirp profiler imaged stratigraphic horizons at a maximum vertical resolution of 0.11 m. AUV navigation was obtained using a Kearfott inertial navigation system and a doppler velocity log.

A dive of the remotely operated vehicle (ROV) Doc Ricketts (DR-134) was conducted on 27 March 2010, prior to the AUV dive in this area. Doc Ricketts was equipped with a vibracoring system and collected four cores using 7.65-cm aluminum core tubes that ranged in length from 95 to 172 cm. The vibracores were logged with a GEOTEK

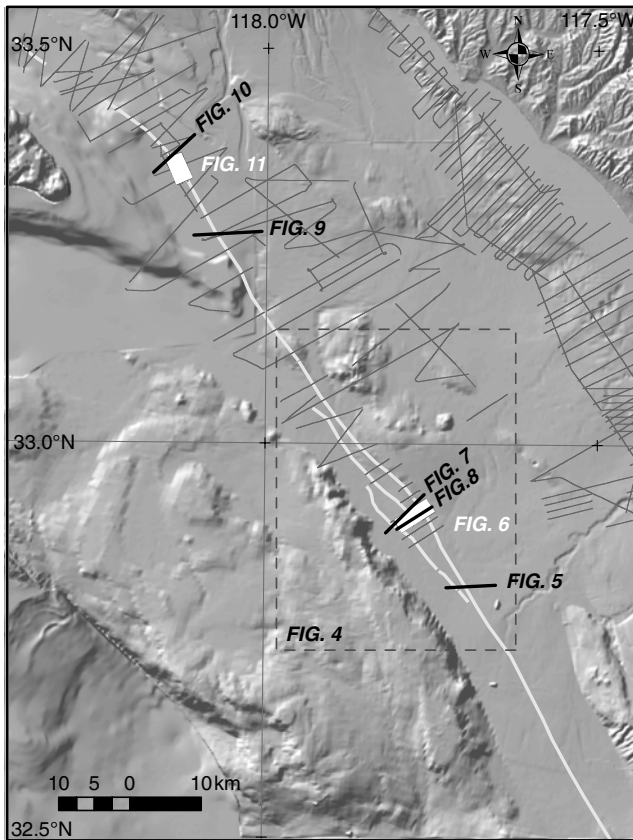


Figure 3. Location of recently (2006–2011) acquired high-resolution minisparker seismic reflection profiles plotted on hillshade of bathymetry. The SDTFZ is shown by white lines. The locations of reflection profiles in this paper are shown by bold black lines with the areas of automated underwater vehicle (AUV) bathymetry shown by white boxes. The dashed box shows the location of Figure 4. The location of figure is shown in Figure 1. See [Data and Resources](#) for the availability of additional reflection profiles used in this study.

multisensor core logger, split, and scanned with a GEOTEK digital line-scanning camera (see [Data and Resources](#)).

Results

Within the confines of the San Diego trough south of La Jolla fan valley, the SDTFZ forms a single principal deformation zone, which at the surface is imaged as either one or two closely spaced fault strands (Fig. 2; Legg, 1991). However, as the SDTFZ approaches the northern end of the trough, the fault zone becomes more complex (Fig. 4). The SDTFZ broadens with a fault strand forming west of and at a 15° oblique angle to the principal strand (Figs. 4 and 5). Reflectors between the fault strands form a broad antiform oblique to both faults; the antiform has little seafloor relief at its southern end (Fig. 5). The seafloor relief increases to a maximum of 50 m as the fault zone broadens to a width of 5 km (Fig. 6). The AUV bathymetry images most of a lozenge-shaped bathymetric high, which we interpret to be a pop-up

structure that formed between the principal strand of the SDTFZ and the newly formed west strand.

The pop-up forms an asymmetric, doubly plunging anticlinorium (Fig. 6). One fold axis trends N80°E and is oriented at a high angle to the main fault strands; the other fold axis trends N40°W, parallel to the main fault strands, and is more tightly folded (Figs. 6 and 7). The AUV multibeam and chirp data show several discontinuous lineations on the surface of the pop-up structure that are primarily at an angle of 30°–50° from the main east and west strands of the SDTFZ (Fig. 6). Some of the lineations show seafloor relief on the order of 5–10 m. A high-resolution minisparker profile collected across the lineations show that at least some of these lineations are surface expressions of faults that show dip-slip (or oblique slip) separation at depth (Fig. 7). Distinctive patches of rough seafloor imaged on AUV multibeam bathymetry are associated with some of these lineations (Fig. 6). Surveys in other areas show that this type of topography is characteristically associated with the occurrence of chemosynthetic biological communities, methane-derived authigenic carbonates, and even active gas venting (e.g., Paull *et al.*, 2008, 2011). Such fluid venting can occur along active fault zones (e.g., Paull *et al.*, 2008).

An industry deep penetration MCS profile that crosses the northern end of the pop-up structure images the main fault strands that define the east and west edges of the pop-up structure (Fig. 8). These strands dip at > 50° near the surface but may become listric at depth. The east-dipping Thirtymile Bank detachment surface intersects the west strand of the SDTFZ, although it is unclear whether the SDTFZ is offset by this surface (Fig. 8). Near the northern end of the pop-up structure, a third high-angle fault strand forms between the east and west strands (Figs. 4 and 8). West of the central strand, the west strand loses its seafloor expression and becomes buried. The central strand is ~20-km long and continues only as far north as Crespi Knoll (Fig. 2). Sparsely spaced minisparker reflection profiles (Fig. 3) suggest that folding between the main SDTFZ faults continues in an en echelon pattern within the stepover, but not as far north as Crespi Knoll (Fig. 4).

West of Crespi Knoll, we mapped a previously unknown continuation of the SDTFZ. While this section of the fault zone has the same orientation as the SDTFZ imaged south of the pop-up structure (N30°W), it is located 5 km to the west (Fig. 2). The newly mapped fault zone is composed of one or two high-angle fault strands (Fig. 9) and extends as far north as the southeastern end of Santa Catalina Island (Fig. 2). A small topographic knoll west of Crespi Knoll is offset in a right lateral sense along this section of the fault zone (Fig. 2). North of the knoll, the fault zone shows increased vertical separation with uplift along the western side of the fault that deforms the seafloor (Fig. 10). At the northern end of the SDTFZ, it crosses the San Gabriel fan valley (Fig. 2). The outer wall of a channel within the San Gabriel fan valley is offset in a right lateral sense (Fig. 11). Within the

Table 1
Radiocarbon Dates for Cores Adjacent to the San Diego Trough Fault Zone

NOSAMS* Accession Number	Core ID	Depth Below Seafloor (cm)	Description	$\delta^{13}\text{C}$	^{14}C Age [†]	Age Error (\pm)	Calibrated Age [†]
OS-87244	DR-134, VC-121	5–8	Mixed planktic foraminifera	1.39	900	25	310
OS-87215	DR-134, VC-121	17–20	Mixed planktic foraminifera	1.10	3,170	25	2,721
OS-87229	DR-134, VC-121	69–72	Mixed planktic foraminifera	1.45	4,290	30	4,088
OS-87230	DR-134, VC-121	121–124	Mixed planktic foraminifera	1.20	5,940	40	6,121
OS-87141	DR-134, VC-123	9–12	Mixed planktic foraminifera	1.67	1,930	25	1,257
OS-87231	DR-134, VC-123	33–36	Mixed planktic foraminifera	1.65	7,200	30	7,468
OS-87142	DR-134, VC-123	47–50	Mixed planktic foraminifera	1.15	8,820	35	9,248
OS-87250	DR-134, VC-123	90–93	Mixed planktic foraminifera	0.41	10,350	45	11,143
OS-87249	DR-134, VC-124	5–8	Mixed planktic foraminifera	1.47	1,010	30	425
OS-87143	DR-134, VC-124	39–42	Mixed planktic foraminifera	1.37	4,670	30	4,609
OS-87232	DR-134, VC-124	124–127	Mixed planktic foraminifera	1.26	8,070	50	8,306
OS-87144	DR-134, VC-125	7–10	Mixed planktic foraminifera	1.64	1,950	25	1,273
OS-87233	DR-134, VC-125	68–71	Mixed planktic foraminifera	1.60	7,030	35	7,326
OS-87234	DR-134, VC-125	128–131	Mixed planktic foraminifera	1.29	10,200	40	10,946
OS-86760	S-12-09-SC, SC-1	4–6	Mixed planktic foraminifera	1.34	875	25	286
OS-87235	S-12-09-SC, SC-1	29–32	Mixed planktic foraminifera	1.67	2,850	35	2,302
OS-86741	S-12-09-SC, SC-1	54–56	Mixed planktic foraminifera	1.61	4,280	30	4,072
OS-87228	S-12-09-SC, SC-1	82–84	Mixed planktic foraminifera	1.72	5,690	30	5,836
OS-86740	S-12-09-SC, SC-1	108–110	Mixed planktic foraminifera	1.03	6,820	40	7,110

*NOSAMS, National Ocean Sciences accelerator mass spectrometry

[†]yr B.P.

crossing of the fan valley, the SDTFZ makes a bend to a more westerly orientation (Fig. 11).

Along its length from the Mexican border to off of Santa Catalina Island, the SDTFZ goes through a restraining stepover and, at its northern end, a restraining bend (Fig. 2). We propose that the changes in orientation along the SDTFZ are controlled by basement structures. Between the Thirtymile and Coronado Banks, the SDTFZ is located in the center of the San Diego trough in the deepest part of the basin between the two basement ridges (Fig. 12). The Coronado Bank only extends as far north as La Jolla fan valley as a bathymetric high (Fig. 2). However, northwest and along strike of the Coronado Bank, a distinct positive gravity anomaly flanks the northeast side of the San Diego trough; this gravity high continues as far north as Crespi Knoll (Fig. 12; Langenheim, 2004). The stepover within the SDTFZ occurs in the narrow (~5 km) area between this gravity high and the gravity high associated with the Thirtymile Bank (Fig. 12). Farther north as the SDTFZ encounters the prominent gravity anomaly northeast of Catalina Island associated with Lasuen Knoll, the fault again bends to the west to a trend of N50°W (Fig. 12).

Miller (2002) modeled a gravity profile across the San Diego trough on a profile that crosses the saddle at the southern end of Crespi Knoll near the northern end of the stepover. This model shows the presence of near-surface (<4 km depth), high-density (3000 kg/m³), high-velocity (6.8 km/s) rock juxtaposed with lower density material across the San Diego trough. The high-density body is modeled to extend from the axis of the San Diego trough in the east to near the base of the continental slope, a distance of about 35 km. This is one of the few places in the Borderland where high-density material is required in the upper crust to match the measured

gravity (Miller, 2002). This high-density material is interpreted to be composed of mafic volcanic rock similar to that dredged from Crespi Knoll (Vedder, 1990). Where the SDTFZ is assumed to encounter this high-density crustal material based on the location of positive gravity anomalies, major restraining stepover or bends formed, indicating basement control of these structures.

Slip Rate on SDTFZ

A slip rate for the SDTFZ is calculated by dating horizontally offset strata of the near-vertical wall of the San Gabriel channel (Fig. 11). The channel wall is offset in two places on the cut-back of a channel meander. The age of the sediment drape that postdates the offset was determined by combining high-resolution seismic reflection profiles and core samples of the channel wall. AUV chirp seismic reflection profiles show a drape of acoustically transparent sediments of 1–3 m thickness that covers both the channel floor and its flanks (Fig. 13). In order to date the base of this layer, we collected one gravity core and four vibracores (Fig. 11). One of the cores (VC-121) was collected from the floor of the main channel. The other cores were collected from outside of but within about 500 m of the channel. Although the cores do not penetrate to the base of the transparent layer, we estimate the age of the base of the layer to be $12,270 \pm 1880$ yr based on sedimentation rates calculated from ¹⁴C ages of foraminifera sampled from within the cores (Tables 1 and 2; Fig. 13). For the calculation of the slip rate, the mean age of 12,270 yr is used as our best estimate of the age of the base of the acoustically transparent layer. The offset of the channel wall was measured at both the north and south channel crossings. This was done by digitally cutting

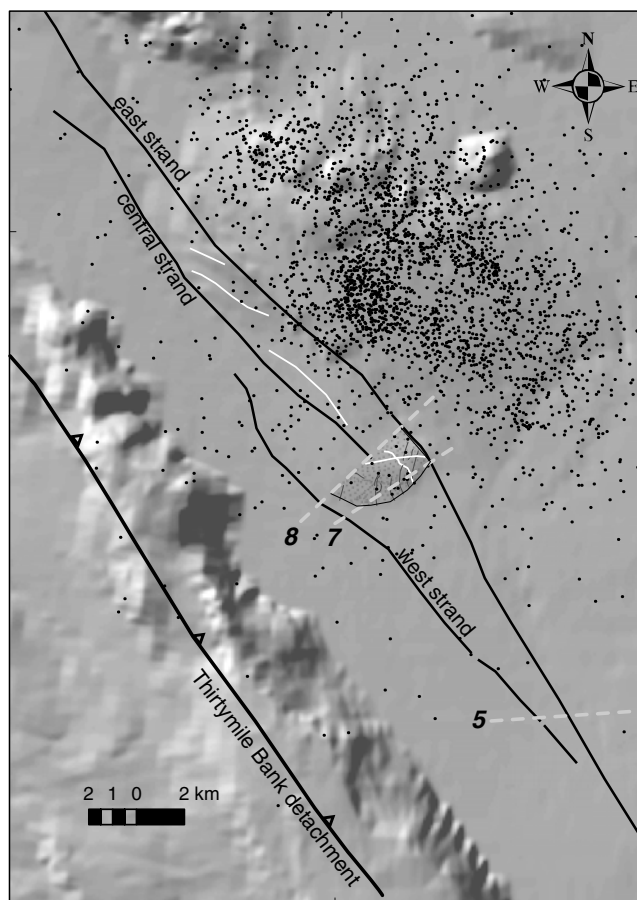


Figure 4. Detailed map of stepover area with fault strands shown in black and fold axes in white plotted on hillshade of bathymetry. Up-dip end of the Thirtymile detachment surface modified from Rivero and Shaw (2011). Black dots show epicenters of the 1986 Oceanside aftershocks (Astiz and Shearer, 2000). Locations of reflection profiles in Figures 5, 7, and 8 are shown by dashed gray lines. The location of the pop-up structure (Fig. 6) is shown by a lightly stippled pattern.

the bathymetric grid along the trace of the SDTFZ and, using a 3D model, restoring the offset until the channel wall was realigned across the fault. Inspection of the model indicates that the offsets of both the northern and southern channel walls are about 18 ± 2 m.

The transition from layered to acoustically transparent reflectivity of the sediments corresponds to a transition from periods of active sediment transport within the channel, layered sediments, to a period dominated by hemipelagic sedimentation, acoustically transparent sediments (Fig. 13). We assume that erosion of the channel wall is dependent on active sediment transport through the channel and that offset of the channel wall postdates active sediment transport in the channel, because down-channel sediment flows are expected to erode away pre-existing offset of the channel walls. There has been little erosional modification of the channel walls by slumping after the channel became inactive, as evidenced by the lack of any significant debris deposits along the base of the channel wall. Therefore, we infer that the apparent offset

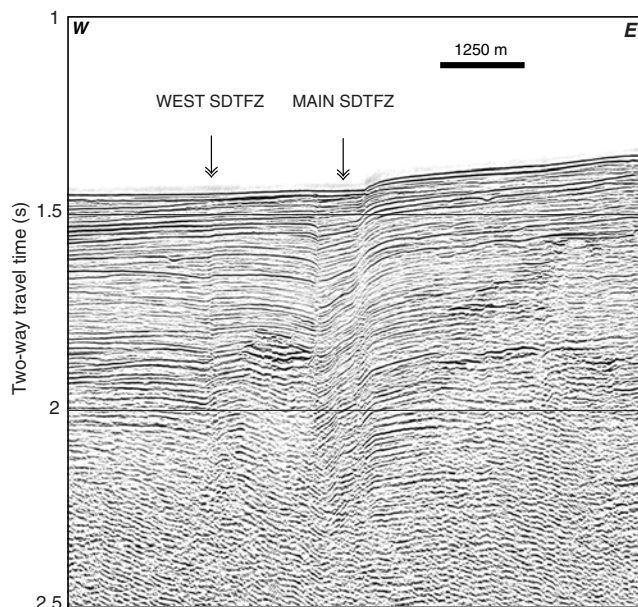


Figure 5. High-resolution MCS profile collected in 1999 (Sliter *et al.*, 2005) across the SDTFZ showing initial formation of stepover (west SDTFZ) on a fault strand about 1.5 km west of the main SDTFZ. This profile is located about 10 km south of the pop-up structure (Fig. 3). Vertical exaggeration is $\sim 3.5:1$. The location of the profile is shown in Figures 3 and 4.

of the channel wall postdates the transition of the San Gabriel channel from active to inactive.

This transition from an active to inactive channel is manifested by the development of an acoustically transparent layer in the seismic reflection profiles that is composed predominantly of hemipelagic mud. The age of the base of this layer thus approximates the age of the undeformed channel wall prior to the development of the observed offset. Using a value of 18 m of strike-slip offset of the channel wall and 12,270 yr as the age when the channel became inactive, this yields a slip rate of about 1.5 mm/yr. Uncertainties in the total amount of offset and in the projection of sedimentation rates indicate an error of ± 0.3 mm/yr. Therefore, we consider the slip rate of the SDTFZ to be in the range of about 1.2–1.8 mm/yr. This slip rate would be at its minimum value if additional subparallel fault strands take up significant slip.

Discussion

The SDTFZ is a linear, right-lateral, strike-slip fault that runs along the center of San Diego trough at a trend of $N30^\circ W$ for approximately 110 km. Based on recently collected seismic reflection profiles, we extend the fault zone an additional 60 km to the north. About 20 km south of Crespi Knoll, the fault zone intersects a topographic and gravity high resulting in a fault bend near the point of intersection (e.g., Mann, 2007). Here, the SDTFZ steps 5 km to the left over a distance of about 20 km. The stepover is complex, involving at least three strands subparallel to the main

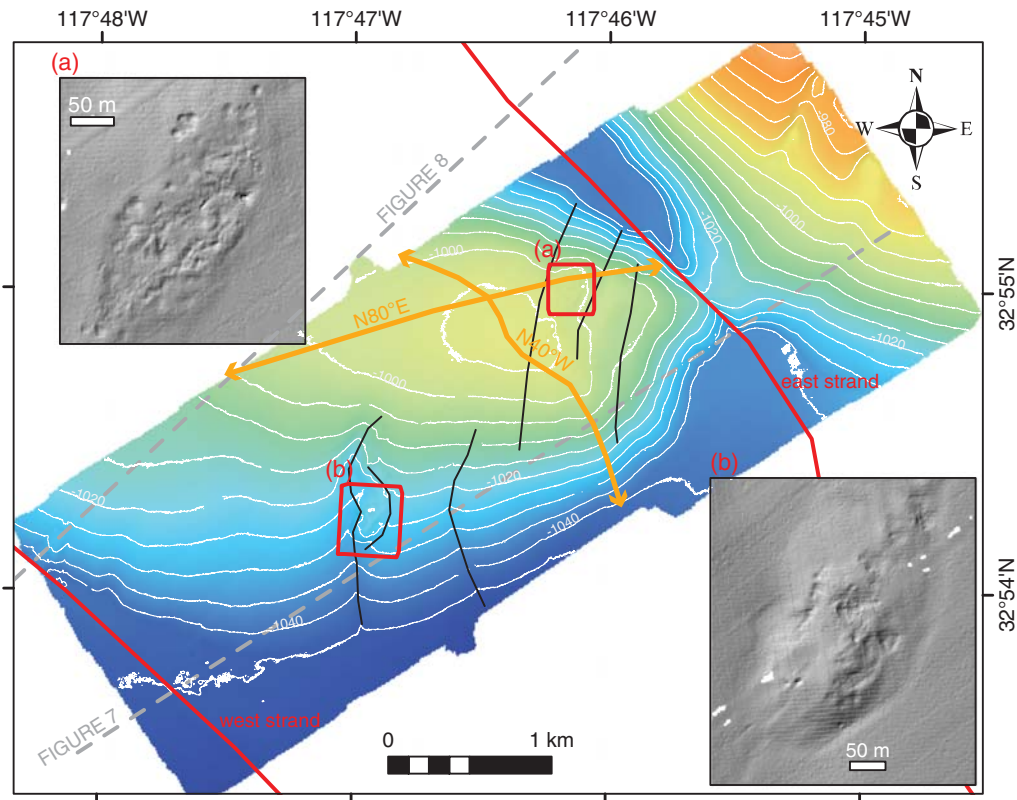


Figure 6. Ultra-high-resolution AUV multibeam data acquired across the pop-up structure between two strands of the SDTFZ (east and west strands shown in red). The pop-up structure is a doubly plunging anticlinorium (fold axes shown in orange). The pop-up is cut by discontinuous oblique faults (shown in black); some of these faults show vertical separation as shown in Figure 7. The contour interval is 5 m. (a, b) The insets show higher resolution images of distinctive patches of rough seafloor that are typically associated with fluid venting; these patches include fault scarps. The locations of Figures 7 and 8 are shown by dashed gray lines. The location of the AUV multibeam survey is shown in Figure 3.

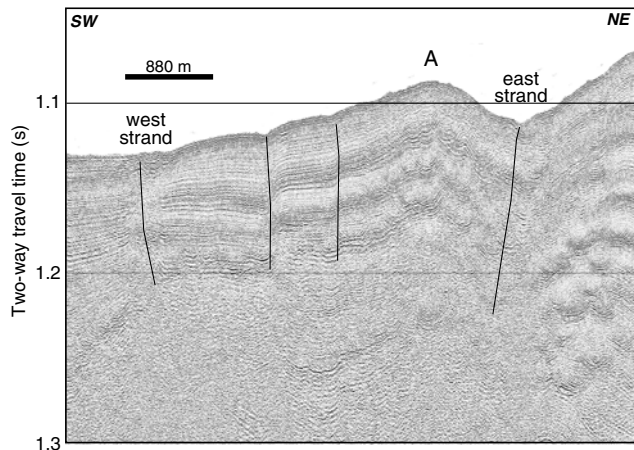


Figure 7. High-resolution minisparker profile collected across the pop-up structure that shows asymmetrical antiform (A) that is subparallel to the main east and west fault traces. High-angle faults are coincident with lineations shown on the AUV multibeam bathymetry (Fig. 6) and show vertical separation. The profile crosses rough seafloor patches shown in Figure 6. The data have been migrated using a constant velocity of 1500 m/s. Vertical exaggeration is about 24:1. The location of the profile is shown in Figures 3 and 6.

SDTFZ with along strike overlap between the fault traces. Some of the deformation is accommodated by dip-slip faults that are oriented oblique to the primary trending zone of deformation (e.g., McClay and Bonora, 2001).

North of the bend in the SDTFZ, it has been proposed that motion along the SDTFZ is transferred to the Catalina fault zone across a 40° restraining bend (Legg, Borrero, and Synolakis, 2004; Legg *et al.*, 2007). The Catalina fault zone runs along the escarpment forming southeast side of Catalina Ridge. Although Santa Catalina Island is uplifted along the Catalina fault zone (Fig. 3), it is less clear whether the fault is still active and accommodates significant strike-slip motion. In a study of the stratigraphy of Catalina basin, which lies immediately west of the fault, Normark *et al.* (2004) show that the youngest basin sediment is not deformed adjacent to the fault. Slightly uplifted beds suggest that the most recent movement of the Catalina fault zone occurred during a sea level lowstand that corresponds with oxygen isotope stage eight (~300 ka). We also collected minisparker reflection profiles across the projected connection between the SDTFZ and the Catalina fault zone in order to confirm the lack of

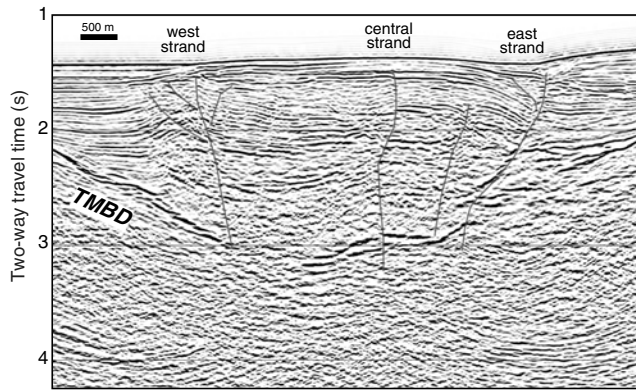


Figure 8. Deep penetration industry MCS reflection profile that crosses the pop-up structure (note the slight bowing of the seafloor). The east and west strands of the SDTFZ are high-angle faults that may become listric at depth. This profile crosses the southern end of the central fault strand, which deforms the seafloor farther north. It is unclear what the relationship is between the Thirtymile Bank detachment (TMBD) and the SDTFZ at depth. Vertical exaggeration at seafloor is $\sim 2:1$. The location of the profile is shown in Figures 3 and 4.

deformation of the youngest sediment (data not shown). It is possible that slip along the Catalina fault zone lies entirely within basement rock outside of the basin. However, submarine terraces surrounding Santa Catalina Island indicate that it is subsiding (Davis, 2004; Conrad *et al.*, 2010) and not uplifting as would be expected if the island were experiencing active transpression. Furthermore, the Catalina escarpment is not associated with significant background seismicity (Hauksson and Jones, 1988).

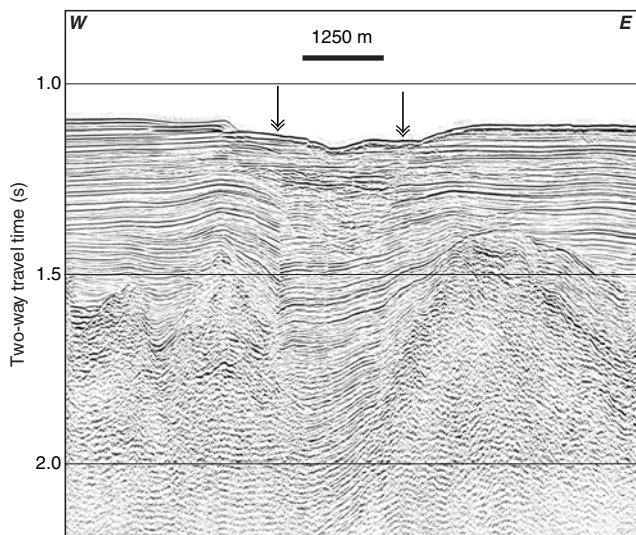


Figure 9. High-resolution MCS reflection profile located east of the southeastern end of the Catalina Ridge. The SDTFZ is composed of two strands that converge at depth. The strands show vertical separation, although the relief on the seafloor is minimal. The fault apparently controls the location of a submarine channel that is located between the two strands. Vertical exaggeration is $\sim 8:1$. The location of the profile is shown in Figure 3.

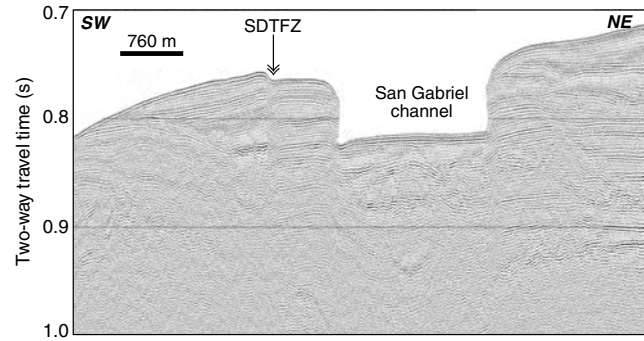


Figure 10. High-resolution minisparker reflection profile immediately north of where the SDTFZ offsets the outer wall of the western San Gabriel submarine channel. Here the fault zone shows dip-slip separation, which is up to the west. It is unclear whether there is another fault strand that runs along the western wall of the channel. Vertical exaggeration is $\sim 19:1$. The location of the profile is shown in Figures 3 and 11.

Using high-resolution reflection profiles, we trace the SDTFZ as far north as the San Gabriel fan valley (Figs. 2 and 11), where the fault bends to the left in a more westerly orientation of about $N50^\circ W$. Northwest of the channel, the SDTFZ is on trend with the SPBFZ, although there is not a simple relationship between these faults (Conrad *et al.*, 2010). A series of western-trending faults and folds deform young sediment in the eastern San Pedro basin between the SDTFZ and SPBFZ (Conrad *et al.*, 2010). Where the SPBFZ has been mapped north of these folds, it shows evidence of recent activity including offset of shallow sediment and arching of the seafloor and is associated with an area of small to moderate earthquakes (Fisher *et al.*, 2003). In addition, diapirs have been mapped within the SPBFZ beneath Santa Monica Bay, which indicate that methane is venting along the fault (Fisher *et al.*, 2003; Paull *et al.*, 2008). The fault continues northwest and intersects the Dume fault near Point Dume on the Malibu coast (Fig. 1; Legg, Kamerling, and Francis, 2004). If the SDTFZ and SPBFZ connect, the combined length of the two fault zones is on the order of 260 km. The possible continuation of the SDTFZ–SPBFZ to the south on the 70-km-long Bahia Soledad fault zone would result in a total fault length of 330 km.

It is unclear whether an earthquake will propagate through restraining or releasing bends along the SDTFZ–SPBFZ–Bahia Soledad fault zone as this will have a significant impact on the potential maximum earthquake magnitude on the fault zone (e.g., Wells and Coppersmith, 1994). The length of a rupture is commonly less than the entire mapped length of a fault, in part, because of the presence of geometric complexities such as restraining bends (Wesnousky, 2006). A stepover width of greater than 5 km is likely to form a barrier to throughgoing rupture, with restraining geometries more likely to form barriers to rupture than releasing geometries (Harris and Day, 1993; Oglesby, 2005; Mann, 2007). Thus, the width of the SDTFZ stepover is at the limit for the dimensions that a fault is likely to stepover. In addition to the

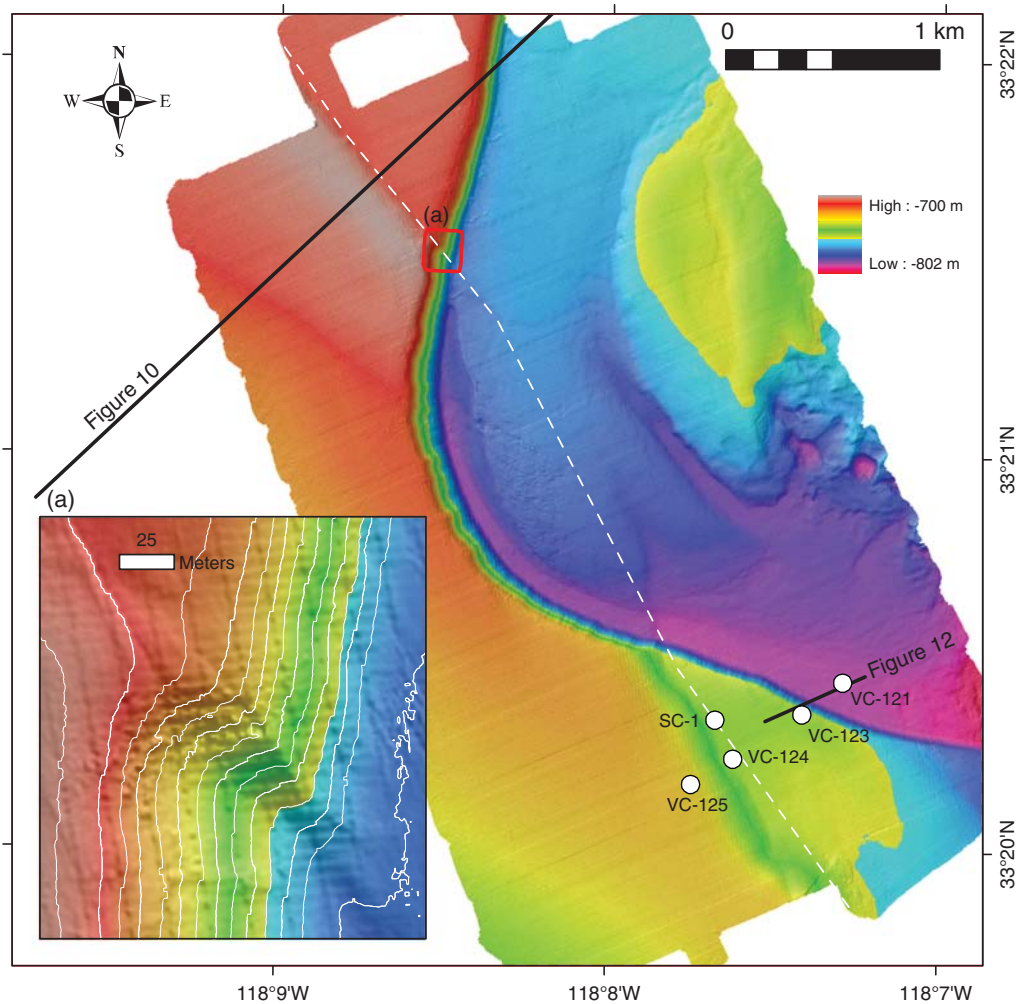


Figure 11. AUV multibeam bathymetry showing offset of the western San Gabriel channel wall in a right-lateral sense along the SDTFZ (shown by a white dashed line). Both the northern and southern offsets of the outer channel wall are about 18 m. (a) The inset shows a close-up of the offset northern channel wall with 5-m bathymetric contours shown in white. The color bar is the same for both the map and the inset. The locations of the cores used to date the offset are shown by white dots.

restraining stepover and bend described in this paper, [Legg *et al.* \(2007\)](#) show additional small restraining bends farther south of Coronado Bank along the SDTFZ. It is unclear whether an earthquake will propagate across these restraining bends and steps. However, the link between the SDTFZ and SPBFZ is composed of a fold belt. If the two faults are linked by reverse faults, it would be more favorable for an earthquake to propagate between the faults ([Oglesby, 2005](#)).

A major implication for the presence of a 20-km-long stepover zone within the SDTFZ is that it allows for an alternate interpretation for the origin of the 1986 Oceanside earthquake swarm. The epicenter of the 1986 Oceanside earthquake is located just north of midway along the stepover zone (Fig. 2; [Hauksson and Jones, 1988](#); [Pacheco and Nabelek, 1988](#); [Astiz and Shearer, 2000](#)). The mainshock had a magnitude of M 5.3 with a reverse focal mechanism oriented N70°W dipping 50° S or N40°W dipping 40° N (Fig. 2; [Hauksson and Jones, 1988](#); [Pacheco and Nabelek,](#)

[1988](#)); many of the aftershocks had strike-slip focal mechanisms ([Hauksson and Jones, 1988](#)). The selection of the southeast-dipping nodal plane would be consistent with the rupture of a left-stepping bend within the right-lateral SDTFZ ([Hauksson and Jones, 1988](#)). The alternate nodal plane is consistent with a northeast-dipping thrust fault, which [Rivero *et al.* \(2000\)](#) and [Rivero and Shaw \(2011\)](#) suggest involves the partial rupture of a reactivated Thirtymile Bank detachment fault as a blind thrust fault.

All of the seismograms recording the Oceanside swarm are located at a minimum distance of 50 km from the epicenter, and thus the depth and location of the aftershocks are generally not well constrained. [Astiz and Shearer \(2000\)](#) relocated the earthquake and its aftershocks and were able to resolve the aftershocks into a shallow plane dipping northeast at 30°. The relocations support the interpretation of the Oceanside swarm as a thrust source. [Rivero and Shaw \(2011\)](#) indicate that the relocated earthquakes occur down-dip of

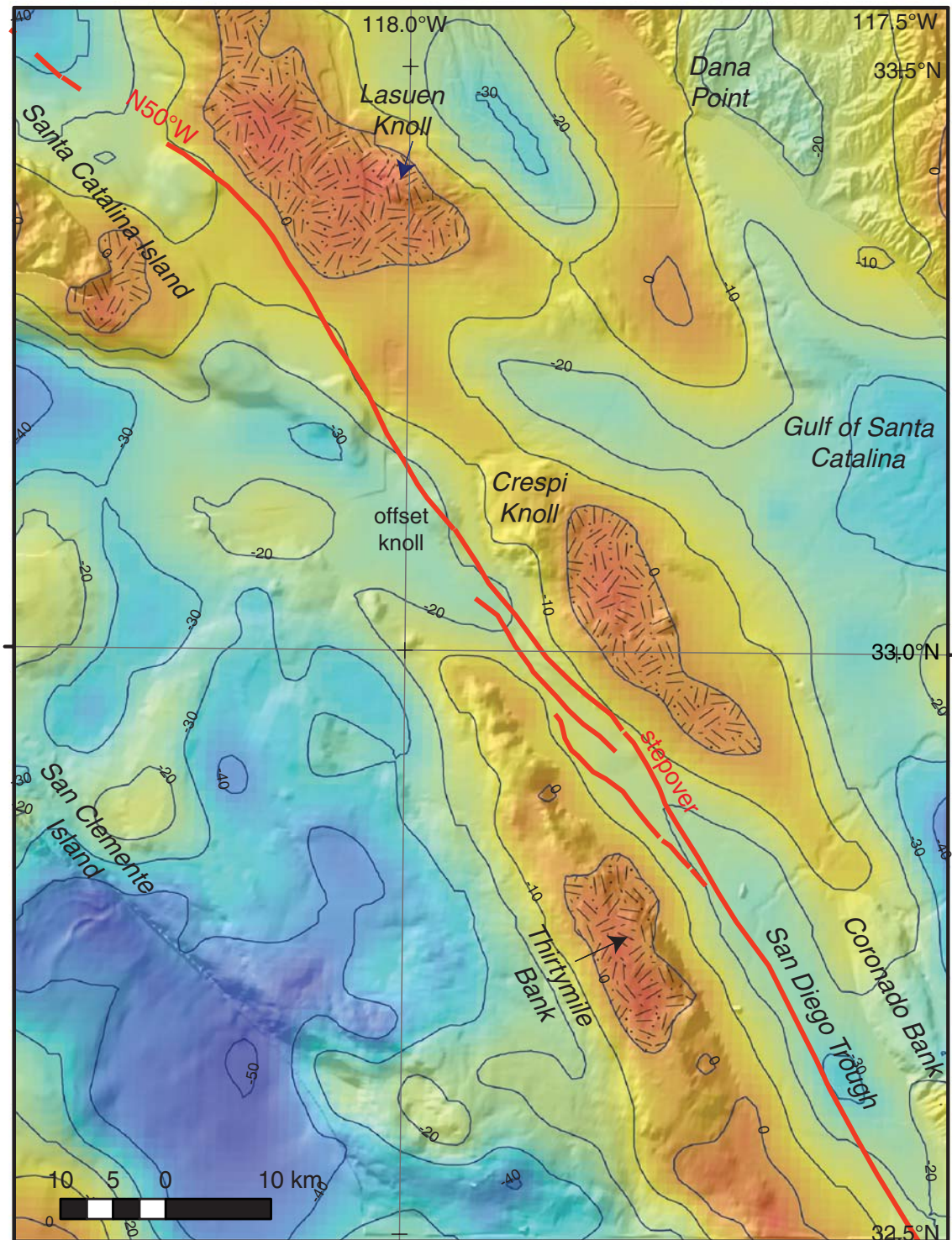


Figure 12. Isostatic gravity anomaly map (Langenheim, 2004) draped on hillshade of bathymetry (the location of the map is shown in Figure 1). A stepover along the SDTFZ occurs between two northwest-trending positive gravity anomalies associated with Thirtymile Bank and a feature southeast of Crespi Knoll. The SDTFZ bends to the left between gravity high associated with Lasuen Knoll and Santa Catalina Island. The contour interval is 10 mGal.

where they map the Thirtymile Bank thrust fault on a seismic reflection profile. Their preferred interpretation is that the SDTFZ does not extend through the entire crust but terminates at the Thirtymile Bank fault. However, the nature of the con-

tact between the SDTFZ and Thirtymile Bank fault remains equivocal based on industry MCS profiles (e.g., Fig. 8).

We offer an alternative scenario in which the Oceanside earthquake swarm occurred within a restraining stepover

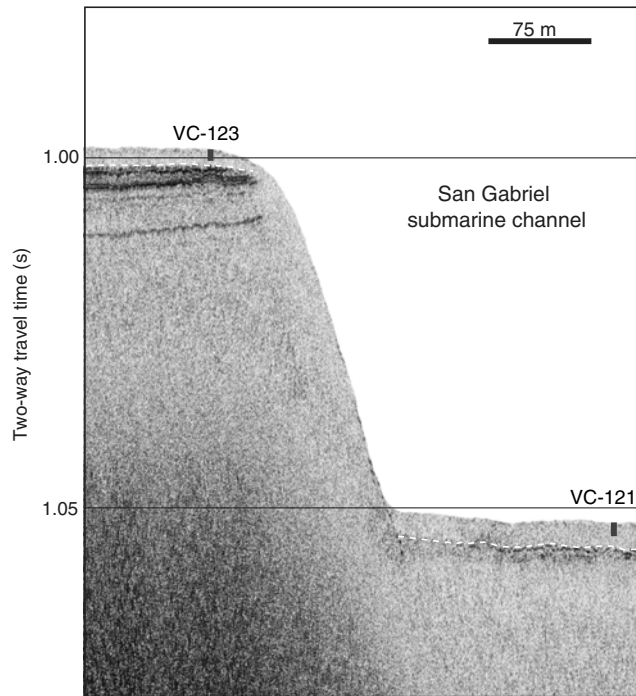


Figure 13. Ultra-high-resolution AUV chirp profile that crosses the channel wall and intersects cores used to determine the age of the base of the acoustically transparent unit. The acoustically transparent layer is best imaged on the channel floor and above the channel wall as delineated by a dashed white line. Vertical exaggeration is about 7:1. The location of the profile is shown in Figure 10.

along the SDTFZ. [Astiz and Shearer \(2000\)](#) state that even the best relocated 1986 Oceanside aftershocks do not form a simple plane but rather outline a 4-km-thick zone of aftershocks. They suggest that this indicates either poor velocity control on the earthquake depths (thus the thick zone) or that the area of aftershocks is within a structurally complex zone, perhaps composed of more than one fault trace. Because the focal mechanism for the mainshock in the Oceanside earthquake sequence was reverse, we suggest that the Oceanside earthquake occurred on a linking reverse dip-slip fault that accommodates transpression within the fault stepover. This could explain the combination of dip-slip and strike-slip aftershocks over a broad area, but it does not explain the overall northeast-dipping cloud of earthquakes. The [Astiz and Shearer \(2000\)](#) relocations were determined using a

1D velocity model. However, as shown by gravity modeling across the San Diego trough ([Miller, 2002](#)), a shallow, high-velocity (~ 6.8 km/s) body lies adjacent to and east of the SDTFZ. In a 1D model, this velocity contrast across the SDTFZ could result in apparently deeper hypocenters east of the fault and thus contribute to the appearance of a dipping cloud of aftershocks.

Conclusions

According to [Meade and Hager \(2005b\)](#), a displacement deficit occurs for offshore faults in the California Borderland when using available fault slip rate models. One fault zone that has not been included in such models is the SDTFZ. We determined a slip rate of about 1.5 ± 0.3 mm/yr over the past 12,270 yr for the SDTFZ and extended the fault northward 60 km via a restraining stepover. We propose that the 1986 Oceanside earthquake swarm occurred within the SDTFZ stepover. It is possible for an earthquake to rupture through one or more restraining bends or stepovers that link the SDTFZ, SPBFZ, and Bahia-Soledad faults, resulting in a potentially larger magnitude earthquake than previously thought. The inclusion of the SDTFZ in the next WGCEP UCERF report should allow for a more accurate assessment of the hazards from offshore faults in southern California.

Data and Resources

Reflection profiles acquired by the U.S. Geological Survey (USGS) are generally available within 2 yr of acquisition. Once the data are published in a USGS open-file report, the data can be downloaded at <http://www.virtualocean.org/> (last accessed March 2011). Industry multichannel seismic (MCS) data have been rescued and archived by the USGS at the National Archive of Marine Seismic Surveys (NAMSS) website <http://walrus.wr.usgs.gov/NAMSS/> (last accessed January 2010). Core logs are archived at the USGS in Menlo Park, California, under Cruise Number W1-10-SC (<http://walrus.wr.usgs.gov/infobank/w/w105sc/>, last accessed September 2011).

Faults not interpreted in this paper can be obtained from the Digital Database of Quaternary and Younger Faults from the Fault Activity Map of California, version 2.0, http://www.conservation.ca.gov/cgs/information/publications/Pages/QuaternaryFaults_ver2.aspx (last accessed December 2006).

Table 2

Sediment Accumulation Rate and Age of Base of Transparent Layer for Cores Adjacent to the San Diego Trough Fault Zone

Core ID	Seismic Line ID	Shotpoint	Thickness of Transparent Layer (ms)	Thickness of Transparent Layer (m)	Sediment Accumulation Rate (cm/ka)	Age, Base of Transparent Layer* (yr)
VC-121	Z110-215	2750	3.50	2.63	19.9	13,191
VC-123	Z110-215	2350	2.13	1.60	15.5	10,306
VC-124	Z110-213	1575	2.94	2.21	15.0	14,700
VC-125	Z110-213	1865	2.31	1.73	16.6	10,437
SC-1	Z110-217	1580	2.76	2.07	16.3	12,699

*Average $\pm 1\sigma = 12,267 \pm 1881$

Acknowledgments

The David and Lucile Packard Foundation provided support for this work. Special thanks are given to the crews of the R/V Zephyr and R/V Western Flyer, the MBARI automated underwater vehicle (AUV) Operations Group, and the MBARI remotely operated vehicle (ROV) pilots. We also thank Dave Caress, Krystle Anderson, and Eve Lundsten for assistance with the multibeam data collection and/or processing. Special thanks also go to the captain and crew for several cruises on the USGS R/V Snavely to collect minisparker and chirp data. In particular, Ray Sliter was instrumental in the collection and processing of the reflection data. Special thanks also go to the staff at the National Ocean Sciences accelerator mass spectrometry (AMS) facility at the Woods Hole Oceanographic Institution for the exceptionally quick turnaround of the ^{14}C data. We also thank Danny Brothers, Chloe Peterson, and an anonymous reviewer for their comments, which significantly improved this paper.

References

- Astiz, L., and P. M. Shearer (2000). Earthquake locations in the inner Continental Borderland, offshore southern California, *Bull. Seismol. Soc. Am.* **90**, 425–429.
- California Geological Survey (CGS) (2006). Digital database of Quaternary and younger faults from the fault activity map of California, version 2.0: http://www.conservation.ca.gov/cgs/information/publications/Pages/QuaternaryFaults_ver2.aspx (last accessed December 2006).
- Caress, D. W., H. Thomas, W. J. Kirkwood, R. McEwen, R. Henthorn, D. A. Clague, C. K. Paull, J. Paduan, and K. L. Maier (2008). High-resolution multibeam, sidescan, and subbottom surveys using the MBARI AUV D. Allan B., in *Marine Habitat Mapping Technology for Alaska: Alaska Sea Grant College Prog.*, J. R. Reynolds and H. G. Greene (Editors), University of Alaska Fairbanks, doi: [10.4027/mhmta.2008.04](https://doi.org/10.4027/mhmta.2008.04).
- Conrad, J. E., H. F. Ryan, and R. W. Sliter (2010). Tracing active faulting in the inner Continental Borderland, southern California, using new high-resolution seismic reflection and bathymetric data (abstract), *Seismol. Res. Lett.* **81**, 347.
- Davis, P. (2004). The marine terrace enigma of Catalina Island—An uplifting experience? in *Geology and Tectonics of Santa Catalina Island and the California Continental Borderland*, M. Legg, P. Davis, and E. Gath (Editors), South Coast Geological Society (SCGS) Guidebook 32, SCGS, Santa Ana, California, 115–122.
- DeMets, C., and T. H. Dixon (1999). New kinematic models for Pacific–North America motion from 3 Ma to present: Evidence for steady motion and biases in the NUVEL-1A model, *Geophys. Res. Lett.* **26**, 1921–1924.
- Field, E. H. (2007). A summary of previous Working Groups on California earthquake probabilities, *Bull. Seismol. Soc. Am.* **97**, 1033–1053.
- Fisher, M. A., V. E. Langenheim, C. Nicolson, H. F. Ryan, and R. W. Sliter (2009). Recent developments in understanding the tectonic evolution of the southern California offshore area: Implications for earthquake-hazard analysis, in *Earth Science in the Urban Ocean: The Southern California Continental Borderland*, H. J. Lee and W. R. Normark (Editors), Geol. Soc. Am. Spec. Pap. 454, Boulder, Colorado, 229–250.
- Fisher, M. A., W. R. Normark, R. G. Bohannon, R. W. Sliter, and A. J. Calvert (2003). Geology of the continental margin beneath Santa Monica Bay, southern California, from seismic-reflection data, *Bull. Seismol. Soc. Am.* **93**, 1955–1983.
- Francis, R., and M. R. Legg (2010). Quaternary uplift and subsidence of Catalina Ridge and San Pedro basin, Inner California Continental Borderland, offshore southern California; results of high-resolution seismic profiling, *Presented at the 2010 Fall Meeting of the American Geophysical Union*, San Francisco, California, 13–17 December 2010, Abstract T13C-2218.
- Gutmacher, C. E., W. R. Normark, S. L. Ross, B. D. Edwards, R. Sliter, P. Hart, B. Cooper, J. Childs, and J. A. Reid (2000). Cruise report for A1-00-SC Southern California Earthquake Hazards project, *U.S. Geol. Surv. Open-File Rept. 00-516*, 50 pp.
- Harris, R. A., and S. M. Day (1993). Dynamics of fault interaction: Parallel strike-slip faults, *J. Geophys. Res.* **98**, 4461–4472.
- Hauksson, E., and L. Jones (1988). The July 1986 Oceanside ($M_L = 5.3$) earthquake sequence in the Continental Borderland, southern California, *Bull. Seismol. Soc. Am.* **78**, 1885–1906.
- Ingram, B. L., and J. R. Southon (1996). Reservoir ages in eastern Pacific coastal and estuarine waters, *Radiocarbon* **38**, 573–582.
- Kennedy, M. P., S. H. Clarke, H. G. Greene, and M. R. Legg (1979). Recency and character of faulting from metropolitan San Diego, California, *Final Technical Rept.—Fiscal Year 1978–1979*, 37 pp.
- Kennett, J. P., E. B. Roark, K. G. Cannariato, B. L. Ingram, and R. Tada (2000). Latest Quaternary paleoclimatic and radiocarbon chronology, Hole 1017E, southern California Margin, in *Proceedings of the Ocean Drilling Program, Scientific Results*, M. Lyle, I. Koizumi, C. Richter, and T. C. Moore Jr. (Editors), Vol. **167**, Ocean Drilling Program, College Station, TX, 249–254.
- Langenheim, V. E. (2004). Gravity and magnetic anomalies of Santa Catalina Island and vicinity, southern California, in *Geology and Tectonics of Santa Catalina Island and the California Continental Borderland*, M. Legg, P. Davis, and E. Gath (Editors), South Coast Geological Society (SCGS) Guidebook 32, SCGS, Santa Ana, California, 277–290.
- Legg, M. R. (1991). Developments in understanding the tectonic evolution of the California Continental Borderland, in *Shoreline to Abyss: Contributions in Marine Geology in Honor of Francis Parker Shepard*, R. H. Osborne (Editor), Society of Economic Paleontologists and Mineralogists (SEPM) Special Publication 46, SEPM, Tulsa, Oklahoma, 291–312.
- Legg, M. R., and M. P. Kennedy (1979). Faulting offshore San Diego and northern Baja California, in *Earthquakes and Other Perils—San Diego Region*, San Diego Association of Geologists (SDAG) Guidebook, P. L. Abbott and W. J. Elliot (Editors), SDAG, San Diego, California, 29–46.
- Legg, M. R., J. C. Borrero, and C. E. Synolakis (2004). Tsunami hazards associated with the Catalina fault in southern California, *Earthq. Spectra* **20**, 917–950.
- Legg, M. R., C. Goldfinger, M. J. Kamerling, J. D. Chaytor, and D. E. Einstein (2007). Morphology, structure and evolution of California Continental Borderland restraining bend, in *Tectonics of Strike-slip Restraining and Releasing Bends*, W. D. Cunningham and P. Mann (Editors), Special Publication 290, Geological Society, London, England, 143–168.
- Legg, M. R., M. J. Kamerling, and R. D. Francis (2004). Termination of strike-slip faults at convergence zones within continental transform boundaries: Examples from the California Continental Borderland, in *Vertical Coupling and Decoupling in the Lithosphere*, J. Grocott, K. J. W. McCaffrey, G. Taylor, and B. Tikoff (Editors), Geological Society Special Publication 227, Geological Society, London, England, 65–82.
- Legg, M. R., V. Wong-Ortega, and F. Suarez-Vidal (1991). Geologic structure and tectonics of the inner California Continental Borderland of northern Baja California, in *The Gulf and Peninsular Province of the Californias*, J. P. Dauphin and B. R. T. Simoneit (Editors), Am. Assoc. Petrol. Geol. Memoir, Vol. **47**, 145–177.
- Lindvall, S. C., and T. K. Rockwell (1995). Holocene activity of the Rose Canyon fault zone in San Diego, *J. Geophys. Res.* **100**, 24,121–24,132.
- Mann, P. (2007). Global catalogue, classification and tectonic origins of restraining- and releasing bends on active and ancient strike-slip fault systems, in *Tectonics of Strike-slip Restraining and Releasing Bends*, W. D. Cunningham and P. Mann (Editors), Special Publication 290, Geological Society, London, England, 13–142.
- McCaffrey, R. (2005). Block kinematics of the Pacific–North America plate boundary in the southwestern United States from inversion of GPS, seismological, and geologic data, *J. Geophys. Res.* **110**, no. B07401, doi: [10.1029/2004JB003307](https://doi.org/10.1029/2004JB003307).
- McClay, K., and M. Bonora (2001). Analog models of restraining stepovers in strike-slip fault systems, *Am. Assoc. Petrol. Geol. Bull.* **85**, 233–260.

- McNeilan, T. W., T. K. Rockwell, and G. S. Resnick (1996). Style and rate of Holocene slip, Palos Verdes fault, southern California, *J. Geophys. Res.* **101**, 8317–8334.
- Meade, B. J., and B. H. Hager (2005a). Block models of crustal motion in southern California constrained by GPS measurements, *J. Geophys. Res.* **110**, no. B03403, doi: [10.1029/2004JB003209](https://doi.org/10.1029/2004JB003209).
- Meade, B. J., and B. H. Hager (2005b). Spatial localization of moment deficits in southern California, *J. Geophys. Res.* **110**, no. B04402, doi: [10.1029/2004JB003331](https://doi.org/10.1029/2004JB003331).
- Miller, K. C. (2002). Geophysical evidence for Miocene extension and mafic magmatic addition in the California Continental Borderland, *Geol. Soc. Am. Bull.* **114**, 497–512.
- Moore, D. G. (1969). Reflection profiling studies of the California Continental Borderland—Structure and Quaternary turbidite basins, *Geol. Soc. Am. Spec. Pap.* **107**, 142.
- Normark, W. R., S. Baher, and R. Sliter (2004). Late Quaternary sedimentation and deformation in Santa Monica and Catalina Basins, in *Geology and Tectonics of Santa Catalina Island and the California Continental Borderland*, M. Legg, P. Davis, and E. Gath (Editors), South Coast Geological Society (SCGS) Guidebook 32, SCGS, Santa Ana, California, 319–334.
- Normark, W. R., J. A. Reid, R. W. Sliter, D. Holton, C. E. Gutmacher, M. A. Fisher, and J. R. Childs (1999). Cruise report for O1-99-SC Southern California Earthquake Hazards project, *U. S. Geol. Surv. Open-File Rept.* 99-560, 60 pp.
- Oglesby, D. D. (2005). The dynamics of strike-slip step-overs with linking dip-slip faults, *Bull. Seismol. Soc. Am.* **95**, 1604–1622.
- Pacheco, J., and J. Nabelek (1988). Source mechanisms of three moderate California earthquakes of July 1986, *Bull. Seismol. Soc. Am.* **78**, 1907–1929.
- Paull, C. K., D. Caress, E. Lundsten, K. Anderson, and R. Gwiazda (2011). Distinctive geomorphology of gas venting and near seafloor gas hydrate sites, *Abstr. Programs Geol. Soc. Am.* **43**, 394.
- Paull, C. K., W. R. Normark, W. Ussler III, D. W. Caress, and R. Keaten (2008). Association among active deformation, mound formation, and gas hydrate growth and accumulation with the seafloor of the Santa Monica Basin, offshore California, *Mar. Geol.* **250**, 258–275.
- Platt, J. P., and T. W. Becker (2010). Where is the real transform boundary in California? *Geochem. Geophys. Geosys.* **11**, no. Q06012, doi: [10.1029/2010GC003060](https://doi.org/10.1029/2010GC003060).
- Rivero, C., and J. H. Shaw (2011). Active folding and blind thrust faulting induced by basin inversion processes, inner California Borderlands, in *Thrust Fault-Related Folding*, K. McClay, J. Shaw, and J. Supper (Editors), *Am. Assoc. Petrol. Geol. Memoir*, Vol. **94**, 187–214.
- Rivero, C., J. H. Shaw, and K. Mueller (2000). Oceanside and Thirtymile Bank blind thrusts: Implications for earthquake hazards in coastal southern California, *Geology* **28**, 891–894.
- Ryan, H. F., M. R. Legg, J. E. Conrad, and R. W. Sliter (2009). Recent faulting in the Gulf of Santa Catalina: San Diego to Dana Point, in *Earth Science in the Urban Ocean: The Southern California Continental Borderland*, H. J. Lee and W. R. Normark (Editors), *Geol. Soc. Am. Spec. Pap.* 454, Boulder, Colorado, 291–315.
- Sliter, R. W., W. R. Normark, and C. E. Gutmacher (2005). Multichannel seismic-reflection data acquired off the coast of southern California—Part A 1997, 1998, 1999, and 2000, *U.S. Geol. Surv. Open-File Rept.* 2005-1084, <http://pubs.usgs.gov/of/2005/1084/> (last accessed November 2010).
- Stuiver, M., and T. F. Braziunas (1993). Modeling atmospheric ^{14}C influences and ^{14}C ages of marine samples to 10,000 BC, *Radiocarbon* **35**, 137–189.
- Stuiver, M., and P. J. Reimer (1993). Extended ^{14}C database and revised CALIB radiocarbon calibration program (version 5.0), *Radiocarbon* **35**, 215–230.
- Vedder, J. G. (1990). Maps of California continental borderland showing compositions and ages of bottom samples acquired between 1968 and 1979, *U.S. Geol. Surv. Misc. Field Studies Map MF-2122*, scale 1:250,000.
- Wells, D. L., and K. J. Coppersmith (1994). New empirical relationships among magnitude, rupture length, rupture width, rupture area, and surface displacement, *Bull. Seismol. Soc. Am.* **84**, 974–1002.
- Wesnousky, S. G. (2006). Predicting the endpoints of earthquake ruptures, *Nature* **444**, 358–360.

U.S. Geological Survey
345 Middlefield Rd., MS 999
Menlo Park, California 94025
hryan@usgs.gov
(H.F.R., J.E.C., M.M.)

Monterey Bay Research Institute
7700 Sandholdt Rd.
Moss Landing, California 95039
(C.K.P.)

Manuscript received 15 November 2011